Numerical study of natural convection in an annulus

Estudio numérico de la convección natural en un anillo

Abrar A. S. Alhadad*, Hussien M. Jassim

University of Babylon-College of Engineering, Mechanical department, Babil, Iraq
* abraralhadad1@gmail.com

ABSTRACT

In this paper, 2-D laminar free convection thermal transmission has been investigated numerically. Double concentric rectangular enclosures with discrete heaters were studied using COMSOL Multiphysics 6.0 software package. Heat flux was applied using specific number of heaters as well as changing the number and distances of the heaters in each case. Heaters were installed on the left vertical wall of the enclosure the opposite wall was kept at constant temperature. The horizontal walls were considered adiabatic. Air was taken as working fluid and all the features of air were considered constant except the change in density due to buoyancy forces that are driving the fluid. Finite volumes method was chosen for solving the governing equations in the dimensionless formula. The effect of Rayleigh number on Nusselt number was analyzed using the resultant isothermal contours. We attained the results for different values of Rayleigh number. A large enhancement in thermal transmission was achieved in the attained results, it was found that the amount of thermal energy transmitted will increase by increasing the value of Ra.

Keywords: free convection; heat source; COMSOL; Air.

RESUMEN

En este artículo, se investigó numéricamente la transmisión térmica por convección libre laminar en 2D. Se estudiaron recintos rectangulares doblemente concéntricos con calentadores discretos utilizando el paquete de software COMSOL Multiphysics 6.0. Se aplicó un flujo de calor utilizando un número específico de calentadores, así como cambiando el número y las distancias de los calentadores en cada caso. Los calentadores se instalaron en la pared vertical izquierda del recinto, mientras que la pared opuesta se mantuvo a temperatura constante. Se consideraron las paredes horizontales como adiabáticas. Se utilizó aire como fluido de trabajo y se mantuvieron constantes todas las propiedades del aire, excepto el cambio en la densidad debido a las fuerzas de flotación que impulsan el fluido. Se eligió el método de volúmenes finitos para resolver las ecuaciones gobernantes en la forma adimensional. Se analizó el efecto del número de Rayleigh en el número de Nusselt utilizando los contornos isotérmicos resultantes. Obtuvimos los resultados para diferentes valores del número de Rayleigh. Se logró una gran mejora en la transmisión térmica en los resultados obtenidos, y se encontró que la cantidad de energía térmica transmitida aumentará al aumentar el valor de Ra (número de Rayleigh).

Palabras claves: Convección libre, fuente de calor, COMSOL, Aire.

1. INTRODUCTION

The study of natural convective mode of heat transfer has drawn the attention of researchers during the last decades due to its significance in lots of engineering fields. Convection mode of thermal transmission in rectangular enclosures added to discrete heaters has enormous relevance due to its role in lots of engineering applications such as cooling microchips (Holman, 2010). The process of thermal energy transmission majorly depends on free convection owing to its straight forwardness, small cost, minimal noise, compact volume, and trust worthiness. The literature review illustrates that the subject of free convective mode of thermal transmission in rectangular geometry has attracted large attention.

Elsayed et al., (2003) investigated experimentally the free convection of air around an elliptic tube with fixed thermal flow. For various Rayleigh numbers and tube inclination angles, the local and average Nusselt number distribution was reported. According to the inward thermal flow, the test Rayleigh number varied from 1.1×10^7 to 8×10^7. For the elliptic tube with straight main axis, the total Nusselt number values were assessed as well as associated with Ra values. Constant heat flux elliptic tubes were compared to free convection around isothermal tubes, and it was discovered which at constant state, the constant thermal flow pipe corresponds well with $Ra^{0.25}$, much like the isothermal tube. Regional Nu allocations as well as the total Nu fluctuation against inclination angle have been used to illustrate how tube orientation affects natural convective thermal transmission. According to the experiment, the tube with a straight main axis was able to reach the highest average Nusselt number. Al-Essa & Al-Hussien (2004) investigated numerically a horizontal rectangular fin with square punctures in both directions dissipates heat by natural convection. The geometrical dimensions as well as perforation orientations are the factors taken into consideration in this study. A comparison of the fin's ability to dissipate heat with various perforation orientations was made. It was discovered that a fin with square perforations parallel to the fin base enhanced heat dissipation more than a fin with slanted square perforations. Using the finite element approach, the study's difficulty was numerically resolved. For a specific range of the perforation dimension, it was discovered that adding square punctures to the fin body raises Surface and thermal losses. Jamal et al., (2008) presented a numerical investigation Using a finite-difference strategy, combined conduction-free convection heat transfers in straight eccentric annuli. For a Newtonian fluid exhibiting a Prandtl number of 0.7, a fluid-annulus radius ratio of 0.5, a solid-fluid thermal conductivity ratio of 10, inner and outer wall dimensionless thicknesses of 0.1 and 0.2, respectively, as well as dimensionless eccentricities of 0.1, 0.3, 0.5, and 0.7, the parameters of the heat transport were presented. Thermal boundary conditions were applied to the annulus walls, which are created by isothermally heating one wall while maintaining the temperature of the funding fluid on the other. TBC were applied to the annulus walls, which are created by isothermally heating one wall while maintaining the temperature of the inflow fluid on the other. For the specified eccentricities, the annulus heights necessary to accomplish thermal complete enhancement were discovered. Additionally, the variation in thermal full development height as a function of eccentricity, a geometrical parameter, was also looked into. The findings shown that raising the eccentricity causes the induced flow rate (F) to raise for a given channel height (L). The overall amount of absorbed thermal energy by the fluid (q) with eccentricity showed a similar trend. likewise, eccentricity boosted the non-uniformity of circumferential temperature as well as the average heat flux values on the interfaces. Sivasankaran et al., (2011) studied a rectangular porous enclosure holding a heat-generating matter, and the impact of discrete heating on free convection heat transmission. The enclosure's right wall was isothermally chilled at a lower temperature, whereas the left wall contained two distinct heat sources. The top and bottom walls as well as the left wall's unheated areas were adiabatic. An implicit finite difference method was used to solve the governing equations'

formulation of the vorticity-stream function numerically. Aspect ratio, Darcy number, heat source length, and modified Rayleigh number were studied as influences on flow and heat transfer. The numerical results showed that when the modified Rayleigh number and the Darcy number grew, the rate of heat transfer boosted but reduced as the aspect ratio increased. In almost all parameter scenarios, with the exception of e = 0.5, it was discovered that the average heat transfer rate was larger at the bottom heater than the above heat source. Additionally, except in the situation where e = 0.5, the maximum temperature was discovered at the bottom heater instead of the usual top heater. The numerical results also showed that the highest temperature increases with aspect ratio and lowers with modified Rayleigh number. Sankar et al., (2011) investigated numerically a geometry where, the upper surface, lower surface, as well as un-warmed portions of the internal surface were insulated, as well as free convective thermal transmission in a cylindrical velar cavity with separate heaters on the internal surface was calculated. The external surface was isothermally chilled at a low T. The distance as well as placement of these isolated thermal sources within the enclosure were altered, and at highest two warming sources at the top and bottom walls were considered to examine the impact of separate heating on free convective thermal transmission. Using a numerical approach and an implicit finite difference method, the governing equations were solved. Analysis was done on how the flow and heat transfer in the annuli were affected by the heater locations, heater lengths, Ar, radii ratio, and modified Ra. The heat transmission rates are higher when the heater is smaller, according to numerical results. It was discovered that the annular cavity's capacity for heat transmission improves with the radii ratio and modified Ra, and that this capacity can be further increased by locating a heater close to the bottom surface. Turan et al., (2012) has done a numerical research on the (CHWF)-induced 2-D steady-state laminar free convective transmission of non-Newtonian inelastic power-law fluids in square enclosures with differentially heated sidewalls. In addition to the simulations, a scaling analysis is carried out to clarify the anticipated impacts of the Nusselt number on the Rayleigh number (Ra), Prandtl number (Pr), and power-law index (n). For nominal values of Ra in the range of 10^3-10^6 and a Pr range of 10-10^5, the effects of n in the range of 0.6 n to 1.8 on heat and momentum transport are examined. The outcomes were also contrasted with those of the constant wall temperature (CWT) arrangement. It was discovered that for both Newtonian and power-law fluids in both configurations, the mean Nusselt number Nu rises with rising values of Ra. However, given equal nominal values of Ra, Pr, and n, the Nu values for the vertical walls subjected to CWHF were lower than the comparable values in the same configuration with CWT. Due to the strengthening (weakening) of convective transport, the Nu values obtained for power-law fluids with (n > 1) were lower than those estimated for Newtonian fluids with the same nominal value of Ra. The mean Nusselt number Nu settled to unity with increasing shear-thickening (i.e., n > 1) as heat transmission occurs primarily by thermal conduction. In the range 10-10^5, the effects of Pr were demonstrated to be basically nonexistent. For both Newtonian and power-law fluids, new correlations for the mean Nusselt number Nu have been put forth. Ahamad et al., (2014) visualized the impact of the viscous dissipation parameter on heat transport by applying heat to the vertical annular cylinder embedded with porous media at three different places. The governing equations were resolved using the finite element method. The effect of the aspect and radius ratios on the Nusselt number was discussed. Streamlines and isotherms were used to illustrate the fluid movement and heat transmission. At larger values of Aspect Ratio Ar, it was discovered that more convection heat transfer occurred at the upper portion of the heated wall of the vertical annular cylinder. With an increase in Radius Ratio Rr, streamline size reduced. Gupta et al., (2016) provided a simulation investigation of the heat transfer caused by free convection in a variety of shaped enclosures. The fixed temperature on the bottom as well as top surfaces, while the side walls were regarded as adiabatic surfaces, was the problem's defining feature. The goal of this study was to determine the shape of enclosure

that would allow for the fastest rate of heat transfer while taking into account various aspect ratio and Grashof umber values. For all enclosures with laminar air flow (at Pr = 0.7), a steady state natural convection issue was developed. Aspect ratio values range from 0.2 to 0.5, whereas Grashof number values range from 10e4 to 10e10. Modelling, simulation, and the conclusion of the study in terms of the Nu were all done using ANSYS 14.0. It was found that heat transfer rate in triangular cavity was more than the rectangular and circular segmented cavity in both cases. Another statement can be concluded that triangular cavity had symmetry of air flow for the lower aspect ratio and low value of Grashof number. While for the higher values (A ≤ 0.3) there was not any symmetry. But for the circular segment cavity there was symmetry for the all cases. In rectangular cavity, it was observed that as aspect ratio decreased, no. of cycles increased as air particles reached cold surface early that higher aspect ratio. The behavior of thermally induced flow of water in an open vertical annulus, circulated through a cold leg producing a closed loop thermo-siphon, was studied numerically and experimentally by (Mustafa et al., 2019). Fluid flow's spatiotemporal behavior was also investigated for a range of heat fluxes. In this investigation, the annuli had Rr of 1.184 and AR of 352 (distance of the test section to annular gap). Experiments were carried out with fixed thermal fluxes of (1-15) Kw/m^2. A 2-dimensional solution was created for computational modeling of the thermal circulation. The experimental data, which included temperature and power supply measurements, was collected using voltage measurement device, current measuring device, and thermocouple. The results showed that the non-dimensional Temp. of H2O increased transiently in the bottom as well as top areas of the annuli over the warmed surface, and that the creation of the TBL starts in the bottom area where warming starts (Seraji & Khaleghi, 2019). A 3-D incompressible laminar circulation through a 270 angle curved velar conduit was quantitatively explored. In toroidal coordinates, the dimensionless governing equations of continuity, momentum, and energy were driven. The projection algorithm was used to discretize the governing equations. The results were acquired using a three-dimensional computer code and a grid generating software written in toroidal coordinates. The solid core had a non-uniform heat source q = BeA, while the exterior wall was supposed to be adiabatic. Taking into account the influence of Re on thermo-hydraulic parameters such as secondary circulation generation as well as axial speed, thermal transmission was raised by utilizing a varied thermal flux rather than constant. The computational outcomes showed that applying a varying thermal flux compared to an unvarying flux raised the average Nusselt number, given that each flux of them has the same value. Furthermore, the outcomes showed that as the aspect ratio was reduced, heat transfer increased.

Aziz & Gaheen (2019) studied free laminar convective flow in an up warded plane of an open, parallel tube with identically heated walls at both ends. The center of the channel, face to face, has an isothermal fin positioned inside the channel's walls. Numerous factors, including the Raleigh number Ra = 5 x10^3–5 x10^6 have been studied numerically. In this work, the effects of these parameters on the flow structure, velocity distribution, temperature domain, and local plus total thermal transmission coefficient have been studied along the channel at various heights. In order to do the numerical analysis, the dimensionless group of heat transfer was employed in the inquiry together with a control volume and the governing PDE. Results revealed that when the fin angle increased, the behavior of the local Nusselt population diminished. It showed that the velocity profiles and temperature distribution along the channel were significantly distorted as the fin length increased. As fin height grew, the heat transmission enhanced and the velocity profiles shrank in the axis. (PATIL, 2020) analyzed fluid flow, heat transfer, and mass transfer in a straight velar cylinder encased in a porous material for the outer wall's convective boundary condition. The assumption was that pure natural convection would be responsible for the fluid movement and heat transfer. A constant temperature was applied to the interior wall. Additionally, it was expected that the species concentration

near the inner wall was uniform. Darcy's law was presumptively observed in the fluid. Using appropriate non-dimensional parameters, the governing partial differential equations were non-dimensional, and finite element analysis was used to find the solution. Triangular components of varying sizes were used to divide the porous material. The linked energy, species, and momentum equations were iteratively solved in MATLAB. For various porous annulus design parameters, the influences of the Ra and Biot number on fluid circulation as well as thermal transmission were examined. The convection was found to raise with the Rayleigh number, according to the results. The radius ratio also increased convection. Additionally, it was found that when the aspect ratio increased, the convection reduced. (Laouira et al., 2020) explored computationally the heater's length influences on the convective circulation in a passage containing trapezoidal geometry. An air circulation at fixed speed and low T entered the passage in a horizontal direction from the. The circulation characteristics were specified as 2-D, laminar and Newtonian. The influences resulting from the heater's size were analyzed. It was discovered that the total (Nu) was raised when the heater's size ascended. Mebarek-Oudina et al., (2020) explored computationally the mixed convective circulation in a horizontally assembled passage containing an opened trapezoidal geometry positioned under it. Air at low temperature entered the passage at constant speed. A thermal source of specified length was embedded on the surfaces of the cavity. Every surface of the passage elsewhere was considered adiabatic. The estimations were done utilizing different positions of the heater. Results revealed that as Ri raised, the total Nu ascended. (Salih et al., 2021) has done an experimental exploration to the free convective thermal transmission in a square geometry containing a porous media as well as warmed unevenly from the lower portion. Thermal transmission across the middle and left portion of the geometry was explored. A fixed thermal flux was utilized during the experiment. The thermal source's placement had a massive effect on the thermal transmission. The outcomes showed that increasing the thermal flux results an increase in the magnitude of Ra as well as Nu. It was concluded that Ra was directly proportional to Nu.

Jamal & Mokheimer, (2022) investigated laminar free convective-conductive thermal transmission in a straight velar passages with inherent eccentricity for the best solid-fluid thermal conductivity ratio and the best cylinder wall thicknesses permitting the highest induced fluid circulation amount as well as thermal transmission under changing geometrical parameters, such as radius ratio and annulus eccentricity. The FDM approach was employed to resolve the PDE for the Prandtl number 0.7 annular fluid and cylindrical annulus walls. For the boundary conditions of single surface warmed isothermally while, the other surface was adiabatic. The ratios of the solid and fluid thermal conductivities and wall thicknesses of the outer and inner circular cylinders, as well as the fluctuations in the induced fluid flow rate and heat transfer in the eccentric annular channel, were obtained. The research used ratios of the solid and fluid thermal conductivities and thicknesses of the cylinder walls that are frequently found. The best conductivity ratio and cylinder wall thicknesses grew nonlinearly with eccentricity and radius ratio, according to the results. These findings can be quite helpful in efficiently constructing the thermal transmission technique for top performance. With different rectangle positioning and thermal features put inside the core of the rectangular enclosure, the current work intends to explore the fluid circulation as well as thermal transmission features. By changing the geometry's placement and the parameter values, a 2-D computational emulation a well as systematic popularization of the free convective thermal transmission behavior occurring in the geometry is performed.

2. MATHEMATICAL FORMULATION

Fig. (1) represents the mesh distribution for the rectangular enclosure having two discrete heat sources. It is hypothesized that the dimension in the z-direction is too large, consequently the influences on the circulation at this direction are neglected, hence fluid circulation as well as thermal transmission are two-dimensional. The top and bottom walls are kept insulated while the right wall is kept at a known temperature. Two separate thermal sources are installed on the left wall. Convective heat transmission is accomplished by passing through the Newtonian fluid, which is incompressible yet extends or retracts in response to temperature variations. The Boussinesq approximation is used as a result of this presumption. The governing equations for steady free convective circulation employing conservation of mass, momentum, and energy may be formulated as long as thermal radiation is disregarded in the aforementioned hypotheses:
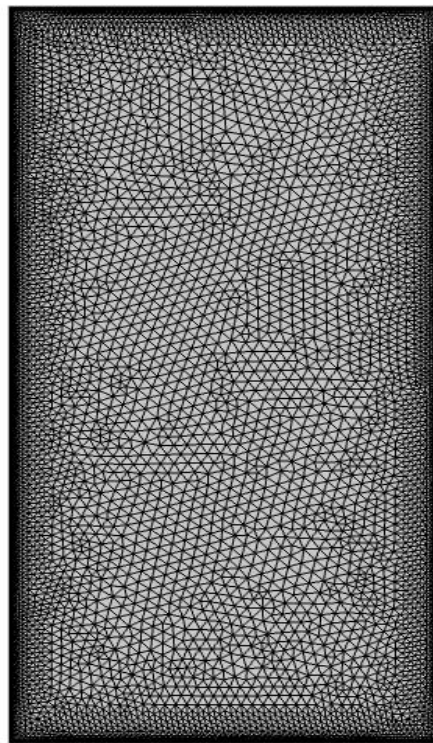
Figure1. Mesh distribution of the physical model in COMSOL.

$$\frac{\partial u}{\partial x} + \frac{\partial v}{\partial y} = 0$$

$$u\,\frac{\partial u}{\partial x} + v\,\frac{\partial u}{\partial y} = -\frac{1}{\rho}\frac{\partial p}{\partial x} + v\left(\frac{\partial^2 u}{\partial x^2} + \frac{\partial^2 u}{\partial y^2}\right)$$

$$u\,\frac{\partial v}{\partial x} + v\,\frac{\partial v}{\partial y} = -\frac{1}{\rho}\frac{\partial p}{\partial x} + v\left(\frac{\partial^2 v}{\partial x^2} + \frac{\partial^2 v}{\partial y^2}\right) + \beta\,g\,(Tf - Tc)$$

$$u\,\frac{\partial T}{\partial x} + v\,\frac{\partial T}{\partial y} = \alpha\left(\frac{\partial^2 T}{\partial x^2} + \frac{\partial^2 T}{\partial y^2}\right)$$

(1)

where the letters f and s, respectively, stand for fluid and solid. All solid-fluid interfaces are believed to be no-slip surfaces. Utilizing the non-dimensional variables below:

$$X = \frac{x}{l}, \qquad Y = \frac{y}{l}, \qquad U = \frac{ul}{\alpha}, \quad V = \frac{vl}{\alpha}$$

$$\Theta f = \frac{Tf - Tc}{Th - Tc}, \qquad P = \frac{pl^2}{\alpha\rho}, \quad Pr = \frac{v}{\alpha},$$

$$Ra = \frac{g\beta\,(Th - Tc)\,\ell 3\,Pr}{v^2}, \qquad \Theta s = \frac{Ts - Tc}{Th - Tc}.$$

(2)

The resulting non-dimensional formula of the equations becomes:

$$\frac{\partial U}{\partial X} + \frac{\partial V}{\partial Y} = 0$$

$$U\frac{\partial U}{\partial X} + V\frac{\partial V}{\partial Y} = -\frac{\partial P}{\partial X} + Pr\left(\frac{\partial^2 U}{\partial X^2} + \frac{\partial^2 U}{\partial Y^2}\right),$$

$$U\frac{\partial V}{\partial X} + V\frac{\partial V}{\partial Y} = -\frac{\partial P}{\partial X} + Pr\left(\frac{\partial^2 V}{\partial X^2} + \frac{\partial^2 V}{\partial Y^2}\right) + Ra\,Pr\,\Theta f,$$

$$U\frac{\partial \Theta f}{\partial X} + V\frac{\partial \Theta f}{\partial Y} = \left(\frac{\partial^2 \Theta f}{\partial X^2} + \frac{\partial^2 \Theta f}{\partial Y^2}\right),$$

$$\frac{\partial^2 \Theta s}{\partial X^2} + \frac{\partial^2 \Theta s}{\partial Y^2} = 0.$$

(3)

The values of the non-dimensional velocity are zero in the solid region and on the solid-fluid interfaces. The boundary conditions for the non-dimensional temperatures are:

$$\Theta f = 1 \ at \ X = 0,$$

$$\Theta f = 0 \ at \ X = 1, \eta$$

$$\frac{\partial \Theta f}{\partial Y} = 0 \ at \ Y = 0, Y = 1,$$

$$\Theta f = \Theta s$$

$$\frac{\partial \Theta f}{\partial \eta} = Kr \ \frac{\partial \Theta s}{\partial \eta}$$

(4)

where $Kr = ks/kf$ is the thermal conductivity ratio.

The movement of fluid is described employing the stream function Ψ obtained from velocity components U as well as V. The relation among Ψ and the velocity components is demonstrated in a single equation as:

$$\frac{\partial^2 \Psi}{\partial x^2} + \frac{\partial^2 \Psi}{\partial Y^2} = \frac{\partial U}{\partial Y} - \frac{\partial V}{\partial X}$$

(5)

The most important physical quantity in this problem is the amount of thermal transmission a swell as distribution can be estimated by applying Fourier's law at the warm surface, as follows:

$$Q = -Kf \ \frac{\partial Tf}{\partial X}$$

(6)

that results in terms of the non-dimensional variables (Roslan et al., 2014):

$$Nuloc = \frac{ql}{(Th - Tc)} = -Kf \ \frac{\partial Tf}{\partial X}$$

(7)

where Nu_{loc} is the local Nusselt number based on ℓ. The local distributions are then integrated to determine the average Nusselt number on the warmed left surface using:

$$Nuavg = \int - \frac{\partial \Theta f}{\partial X} \ dY.$$

(8)

3. COMPUTATIONAL MYTHOLOGY

The CFD program COMSOL Multiphysics 6.0 solves the governing equations and boundary conditions numerically. A FEM solver as well as simulator software package for diverse physics as well as engineering applications is COMSOL Multiphysics (formerly FEMLAB) (Multiphysics, 2013). The Incompressible, two- dimensional laminar flow with heat transfer is described by the isothermal contours resulted from solving the governing equations of the flow. Here the convergence criterion was specified to 10^{-6}.

In the current research, triangles are used to create a mesh for a rectangular enclosure. Fig.1 displays the dispersion of the triangular mesh. To check whether the mesh scheme is adequate and to assure that the outcomes are grid independent, several grid sensitivity tests were performed (Hågbo et al., 2019). For predetermined mesh sizes, we use the COMSOL default values. During examination, the parameters were considered as follows: pr $= 0.71$, $A = 2$, Ra $= 10^5$, and $Kr = 1$ as shown in Table 1.

Table 1. Mesh test

Predefined mesh size	Mesh elements	Average Nusslet	CPU times
Extremely coars	260	18.112	2
Extra coars	460	18.134	2
Coarser	678	18.254	2
Coars	1310	18.432	2
Normal	1975	18.523	2
Fine	2972	18.567	3
Finner	8874	18.621	4
Extra fine	24833	18.633	6
Extremely fine	32445	18.732	7

For all the computations carried out in this research, a finer mesh size was chosen while taking the computation time into account. In order to verify the computational code, the previous published problems on natural convection in a vertical annulus with discrete heat sources were validated.
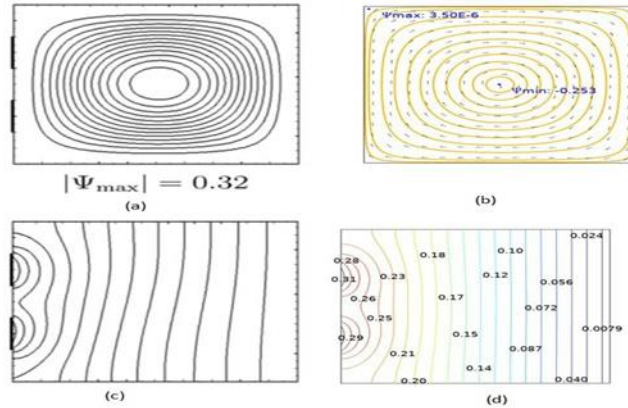
Figure 2. Comparison of the present computed isotherms and stream function (a, c) against that S.Mani et al.(Sivasankaran et al., 2011) for Ra=10^7 in a cylindrical annular cavity with two separate heaters.

The comparison reveals that it agrees with the research that were mentioned. These extensive verification efforts proved how reliable and accurate the current computation is.

4. FINDINGS

The exploration in the undergoing computational analysis are attained in the following range of the dimensionless parameters: the solid rectangular enclosure area, $0 \leq A \leq 2$ and the Rayleigh number, $10^3 \leq$ Ra $\leq 10^7$. The positioning is fixed as vertical installation. Figure 3 illustrates the streamlines. The thermal conductivity ratio is fixed at $Kr = 1.0$ and the Rayleigh number at Ra $= 10^5$. The fluid temperature adjoining the hot surface rises and moves from the left to the right, falling along the cold surface, then rising again at the hot surface. This movement creates a clockwise circulation cell in free space. We investigated the size as well as the placement influences of the separate heaters on the fluid's circulations as well as free thermal transmission aspects in the velar space, considering the following cases:

- ❖ Case I: two separate heaters equal in length s ≥ 0.2.
- ❖ Case II: three discrete heaters equal in length s ≥ 0.1.
- ❖ Case III: three discreet heaters in different lengths0.1 ≤ s ≤0.2.

Plotting the streamline and isotherm contours in the enclosure will show an exemplary flow pattern and the accompanying heat transfer rates for the various situations. Additionally, the changes in the maximum temperature at the heaters will be thoroughly explored, and the amount of thermal transmission at the thermal sources will be reported in terms of regional as well as total Nu.
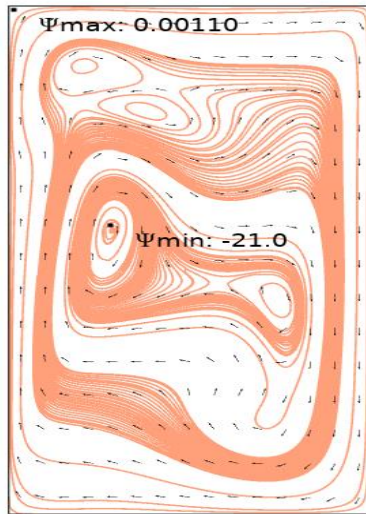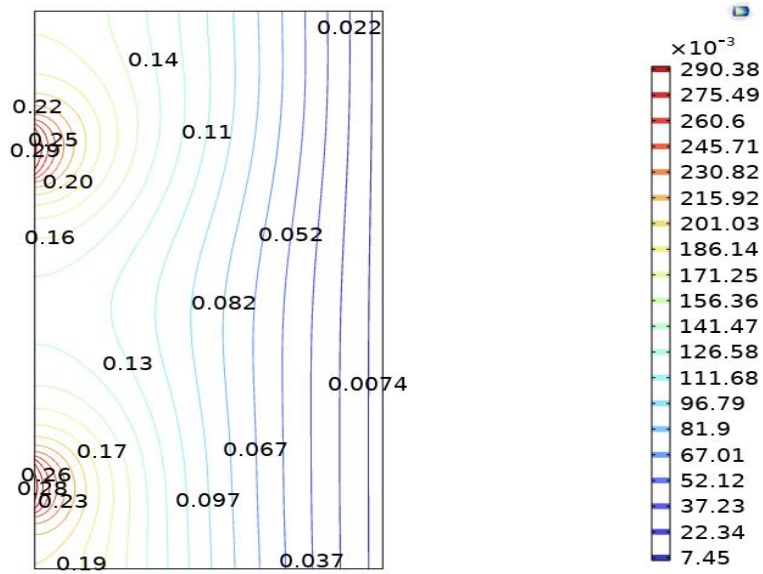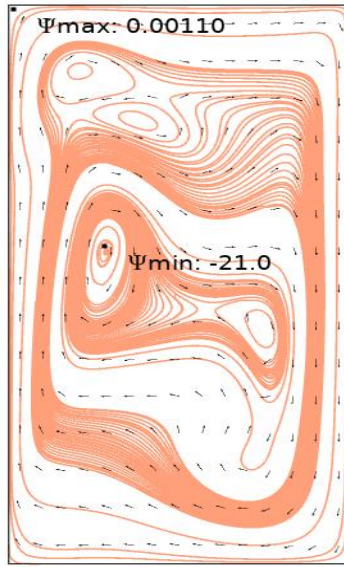
(a)Ra=10^3

Figure 3a. Streamlines and isotherms when Ra = 1e3 for Case I: two discrete heaters equal in length s ≥ 0.2
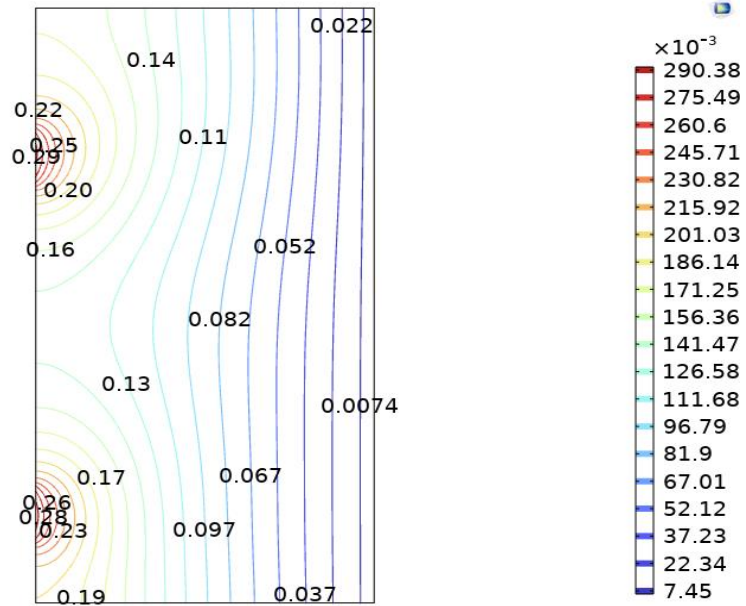
(b) Ra = 10^7
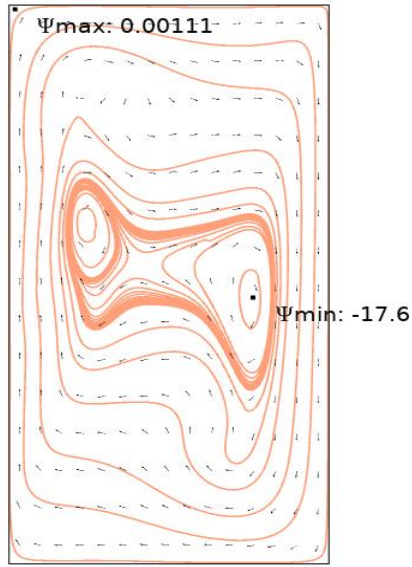

Figure 3b. Streamlines and isotherms when Ra = 1e7 for Case I: two discrete heaters equal   in length s ≥ 0.2
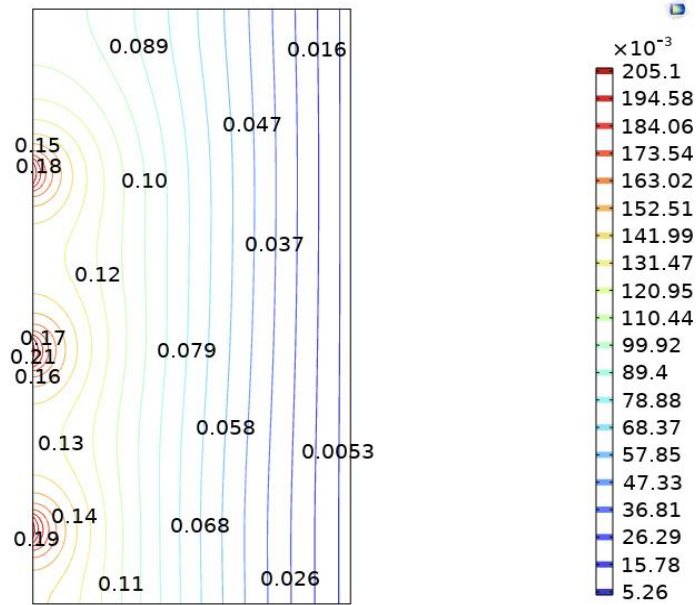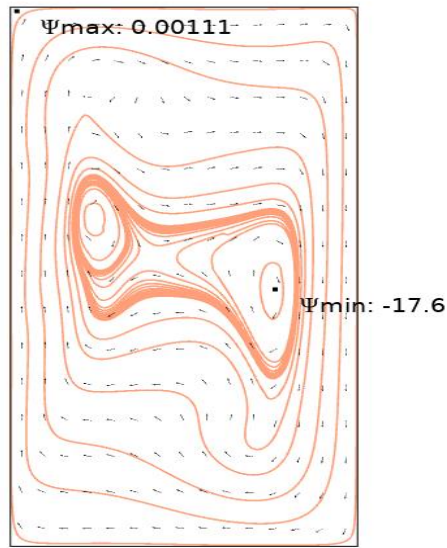
(a)Ra $= 10^3$

Figure 4a. Streamlines and isotherms when Ra = 1e3 for Case II three discrete heaters equal in length s ≥ 0.1.
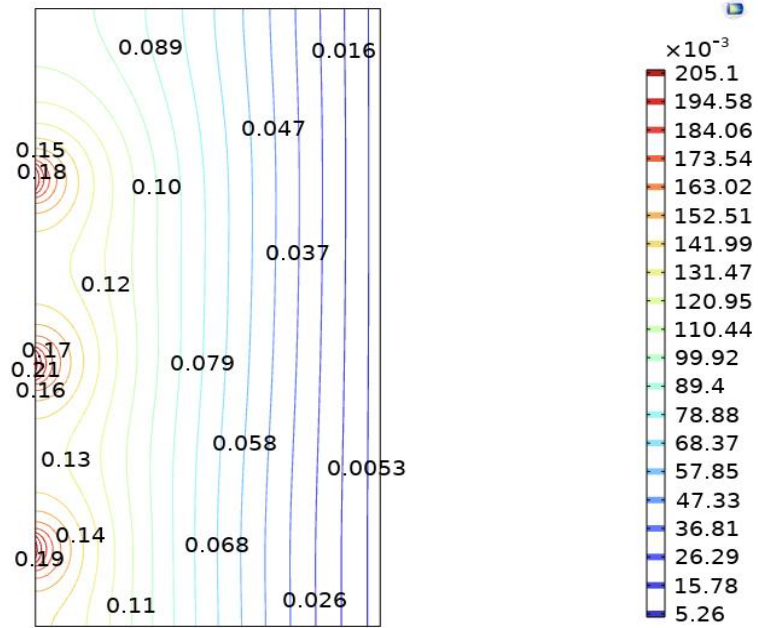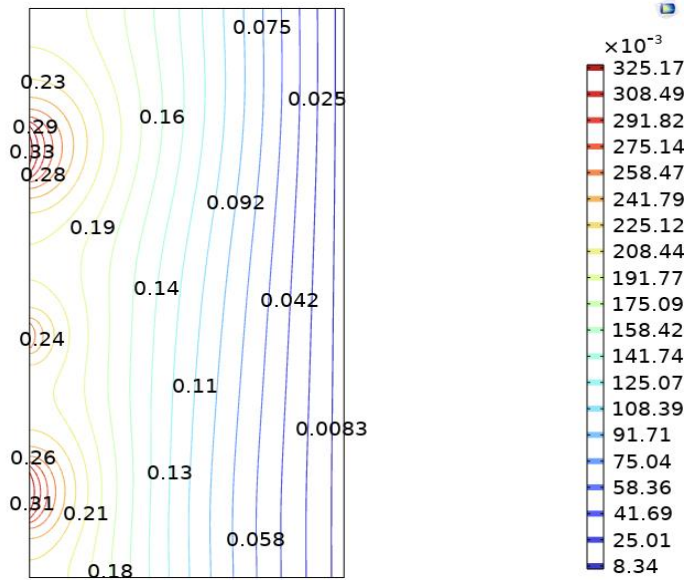
(b) Ra = 10^7
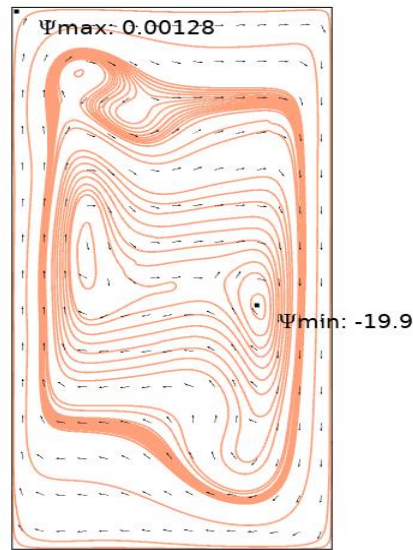

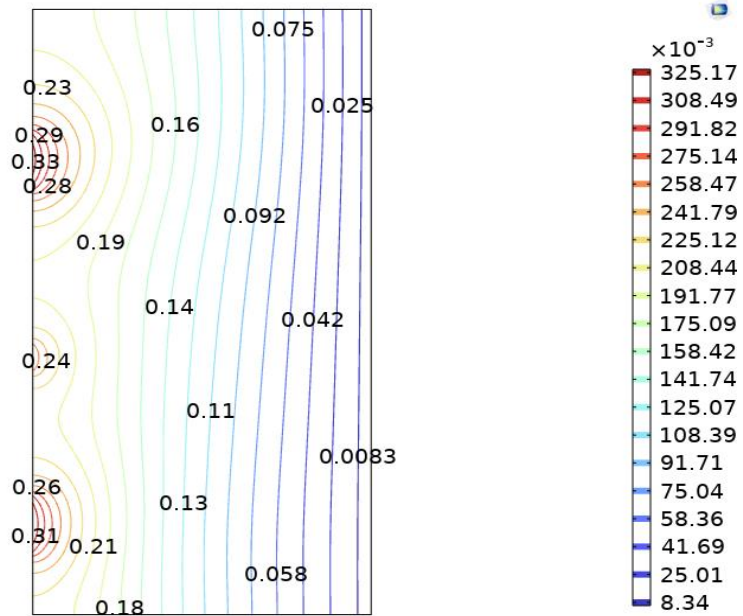Figure 4b. Streamlines and isotherms when Ra = 1e7 for Case II: three discrete heaters equal in length s ≥ 0.1.

(a) Ra = 10^3

Figure 5a. Streamlines and isotherms when Ra = 1e3 Case III: three discreet heaters in different lengths $0.1 \leq s \leq 0.2$.

(b) Ra = 10^7

Figure 5b. Streamlines and isotherms when Ra = 1e7 Case III: three discreet heaters in different lengths $0.1 \leq s \leq 0.2$.

For case I, when low Rayleigh number Ra = 10^3, as shown in Fig. (3a), The relatively undistorted isothermal lines for all of the separate heaters show that the conduction mechanism dominates heat transfer from these devices, as well as a revolving flow sequence around the core of the annulus was observed. In other words,

the fluid is propelled higher by the inner wall's heater and subsequently lower to 10^7 fig.(3b), the flow pattern in the streamlines is stronger, and the annulus's temperature stratification may be seen on isotherms. The internal swirl flows towards the annulus' external surface with an accumulation in value at this high Rayleigh number, a feature that is also reflected in the associated isothermal pattern. It is obvious that the Rayleigh number has a significant impact on the flow and thermal fields. For Case II: three discrete heaters equal in length s ≥ 0.1, fig. (4a, b) when Ra = 10^3, [107] we can see that the intensity of the stream lines has decreases when the using three heat sources at the same length. The stream function's highest value reveals that the main vortex's flow strength decreases. Also we can see that the values on the isotherms has decreased when the length of the heaters are equal. On the other hand, for case III: three discreet heaters in different lengths 0.1 ≤ s ≤0.2, as the size of the lower and top heaters is ascended, the convective circulation in the velar space is improved, and the production of a secondary swirl is seen Fig. 5a. When the bottom and top heater lengths are raised, the isothermal lines have propagated throughout the whole velar space. Additionally, the temperature patterns visualized show the presence of dense isothermal lines close to the thermal source surface, which denotes the formation of TBL. The position of the heater has a significant impact on how the isotherms migrate. where the TBL is visible near the heater.

Generally, we can see that the stronger intensity of the stream lines and the highest value of the stream function were observed at the first case when using two heaters with equal length, whereas the weakest intensity of stream lines and flow pattern was represented in Case II when using three heaters at the same length.

On the other hand, it was obvious that the flow pattern in Case III was better than

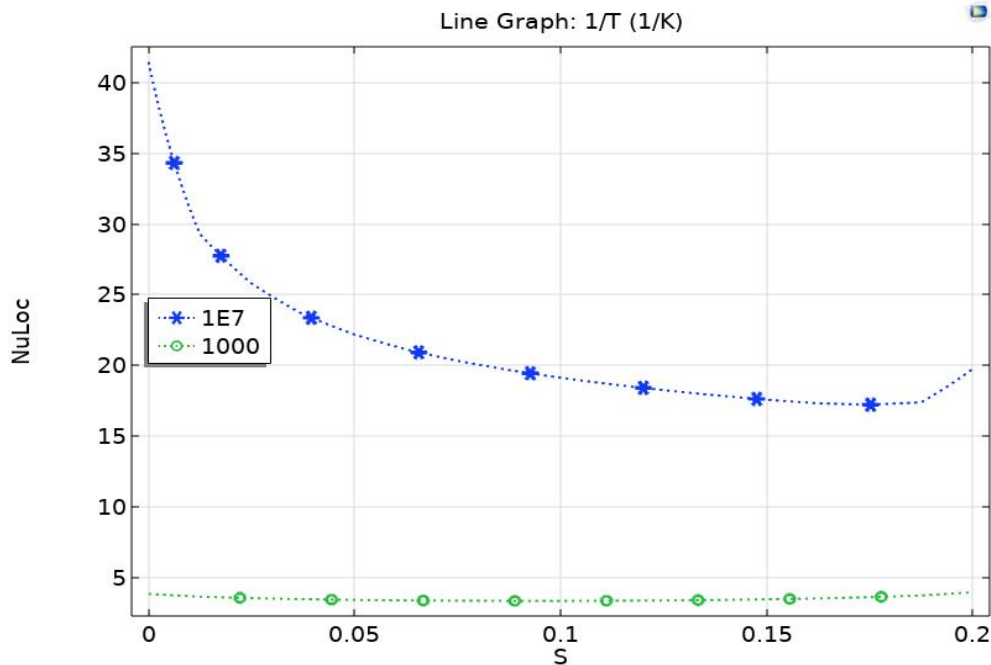Case II. The intensity of the flow is stronger than Case II.

Figure 6. Represents the local Nu number for case I (2 heaters equal in length s=0.2)

In the graph above, fig.6 we can see that there is a significant enhancement in the magnitude of Nuuslet number which is considered as an important indication to the rate of the heat that is transmitted. This enhancement goes together with the increase in the magnitude of Rayliegh number. When taking a small value of Rayliegh number Ra = 10^3 we can see that the value of Nu is very limited, on the other hand when we consider the high value Ra = 10^7 we can see that an enormous increase in the value of Nu takes place which means that Nu is directly proportional to Ra.
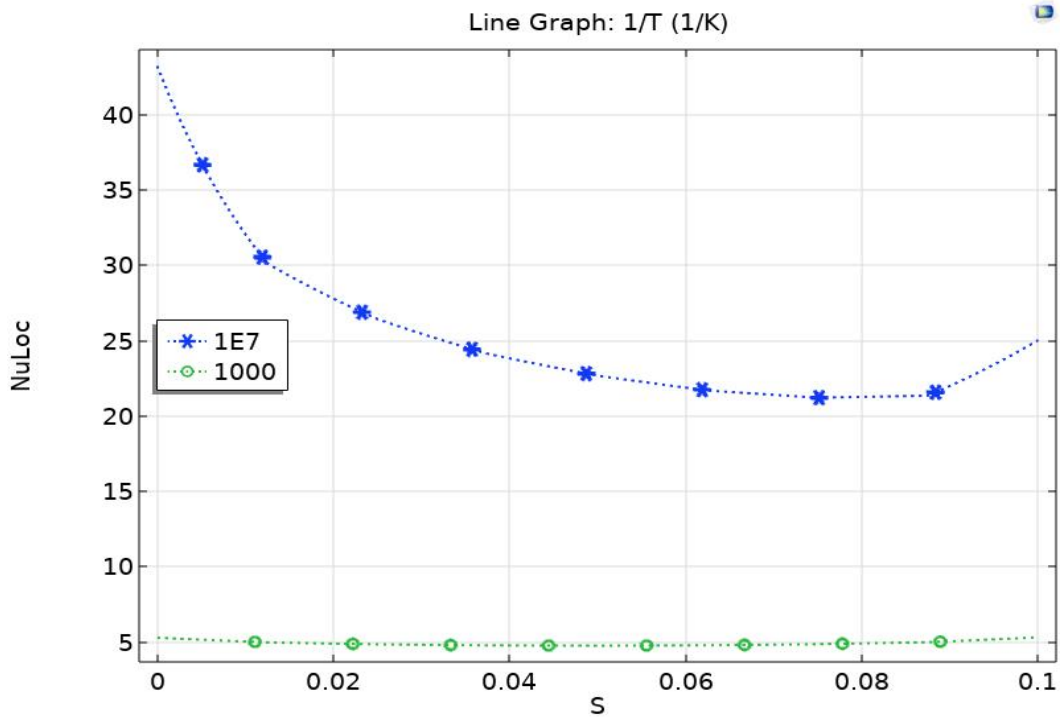

Figure 7. Represents the local Nu number for case II (3 heaters equal in length s=0.1)

Similarly, we can see in fig.7 that the local Nusslet number is directly proportional with Ryleigh number. This graph is a representation for case II where we have 3 heaters at the same length s = 0.1 and it shows the relationship between Nusslet number and Rayliegh number for this case. Unlike the previous case we can observe that the smallest value of Nusslet number is larger than the one in the previous case which means that there is an influence of the length of the heater on the value of Nusslet number. Considering short distance of heat source s = 0.1 the smallest value of Nu = 21 while in the previous case when the size of the thermal source was s = 0.2, the smallest value of Nu equaled to 17.5. Consequently, we attained a better result for the rate of heat transfer which is represented by Nusslet number, by decreasing the value of the heater length to s = 0.1.
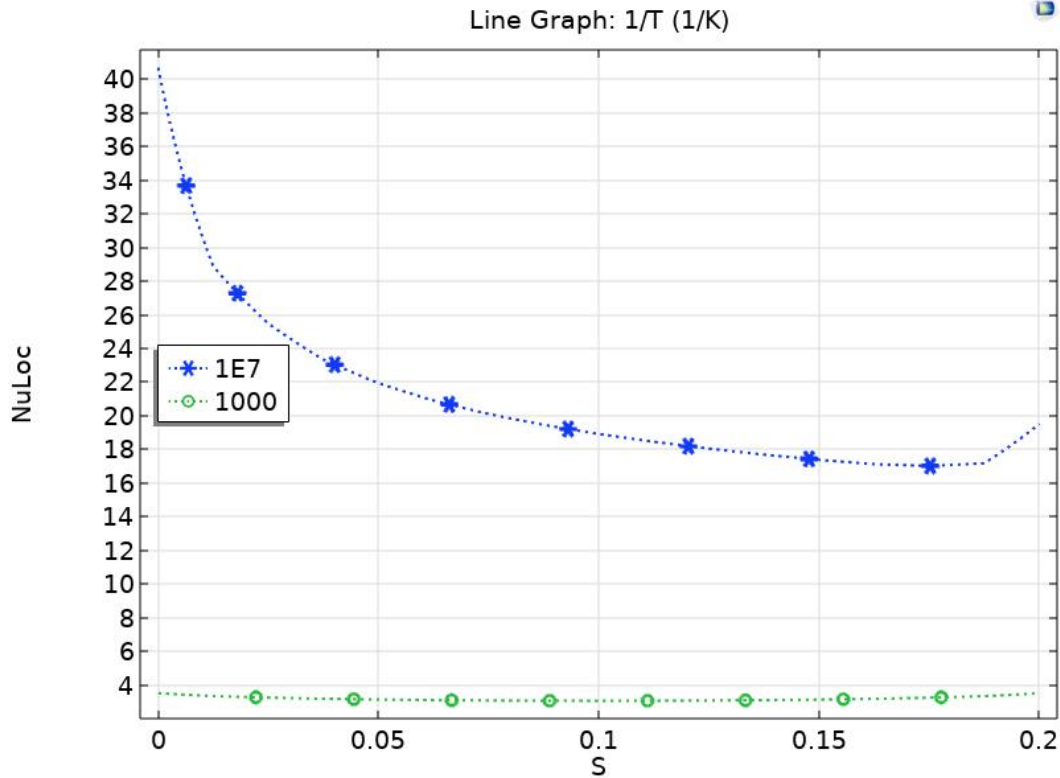
Figure 8. Represents the local Nu number for case III (3 heaters distinct in length s=0.1,0.2)

We can also see in this case that the Nusslet number increases with the increase of Rayliegh number according to the displayed values of Rayliegh number Ra = 10^3 and Ra = 10^7. In this case we have a mixed length of the heaters s = 0.1 and s = 0.2. It is noticeable that the values of Nusslet number in this case is intermediate. Where the smallest value of Nusslet number is 17 while it stabilizes at 20.
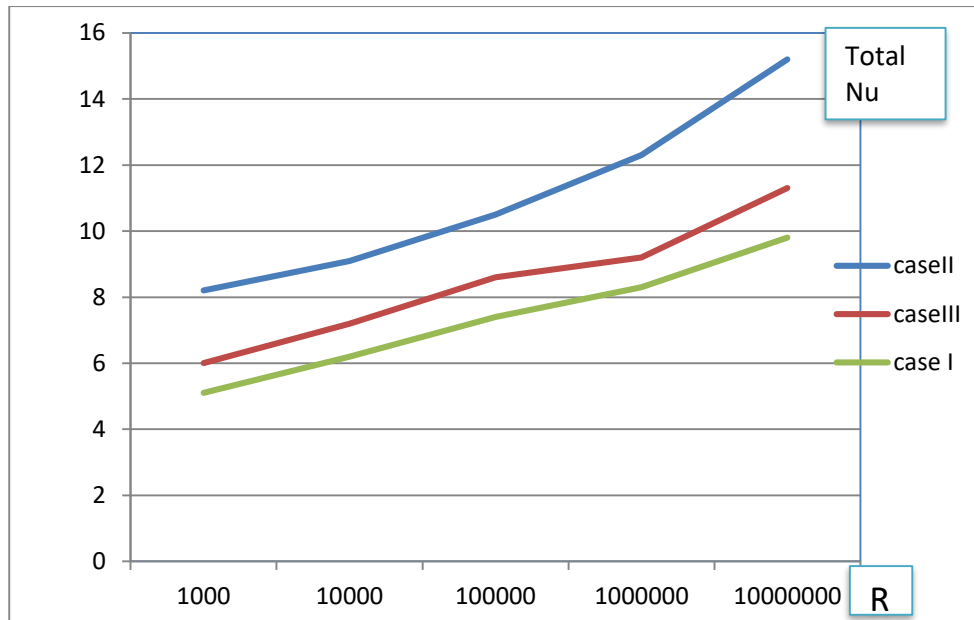
Figure 9. Represents the relationship between the Total Nusslet number for   each case (case I, II, III) with Rayliegh number.

Fig.9 above shows the association between the total amount of transmitted thermal energy represented be total Nuuslet number and Rayliegh number. It was obvious that there is direct proportion between these two parameters by noticing the obvious increase in the total amount of thermal deportation with the value of Rayliegh number, but it was noticed that this total amount of heat represented by total Nusslet number also dependent on the length of the heat source. It is noticeable that the best result was achieved in the second case (case II) considering small and equal length for all heaters in this case (s= 0.1), while the third case achieved intermediate results using two distinct lengths for the heaters (s= 0.1,0.2). Lastly, the least results were accomplished by case I (S=0.2).

According to the illustrated results in the graph above, it was observed that the best case among three cases was the second case with the smallest size of the thermal source s = 0.1, then the third case comes afterwards using distinct lengths of the heaters and at the end come case I with the least results compared to the other cases.

5. CONCLUSION

In this study, a numerical investigation was accomplished to analyze the process of convective thermal transmission in a rectangular enclosure with embedded heat sources on the inner wall. Three different cases were considered and studied in this paper according to the length and locations of these heat sources. The physical model was accomplished utilizing COMSOL 6.0 software package to solve the equations and attain the numerical results. The eventual isothermal contours and streamlines were analyzed accurately to show the results. A noticeable enhancement in thermal transmission was achieved through this work. There was always a direct proportion between Rayliegh number and Nusslet number which means by increasing Ra the value of Nu will increase. Knowing that total Nu represents the total amount of thermal transmission, consequently accomplishing higher values of Nu means a better performance for removing the undesirable thermal energy. Furthermore, it was observed that the length of the heat source has a direct influence on the rate of thermal transmission, a short and equal length for the heaters produces the best rate of heat transfer which is represented be Nusslet number. Using different lengths of heaters (not equal) will give a moderate

1002

results of the amount of heat transmission. The appliance of large length for all the heat sources will reduce the desirable results.

ABBREVIATIONS

Ar: Aspect ratio
S: length of the heater
g: Gravitational acceleration
Kr: Thermal conductivity ratio
k: Thermal conductivity
ℓ: Width and height of enclosure
Nu regional: regional Nusslet Number
Nu $_{avg}$: Total Nusselt number
Ra: Rayleigh number
T: Temperature
TBL: Thermal boundary layer
Pr : Prandtle number
u, V: Velocity components in the x- and
y-directions
x, y&X, Y: Space coordinates & dimensionless space
coordinates.
Greek Symbols
α: Thermal diffusivity
β: Thermal expansion coefficient
Θ: Dimensionless temperature
v: Kinematic viscosity.
Ψ: stream function
Subscript
c: Cold
f: Fluid

REFERENCES

Ahamad, N. A., Arabawy, H. A. M. H. E. L., & Ahmed, S. I. (2014). *INTERNATIONAL JOURNAL OF ENGINEERING SCIENCES & RESEARCH TECHNOLOGY Visualization of Natural Convection in a Vertical Annular Cylinder with a Partially Heat Source and Viscous Dissipation*.

Al-Essa, A. H., & Al-Hussien, F. M. S. (2004). The effect of orientation of square perforations on the heat transfer enhancement from a fin subjected to natural convection. *Heat and Mass Transfer*, *40*(6–7), 509–515.

Aziz, M. A., & Gaheen, O. A. (2019). Effect of the isothermal fins on the natural convection heat transfer and flow profile inside a vertical channel with isothermal parallel walls. *SN Applied Sciences*, *1*(10), 1310.

Elsayed, A. O., Ibrahim, E. Z., & Elsayed, S. A. (2003). Free convection from a constant heat flux elliptic tube. *Energy Conversion and Management*, *44*(15), 2445–2453.

Gupta, A., Thakur, H. C., & Vats, B. (2016). Study of steady natural convection with laminar flow in the enclosures of different shapes. *ASME International Mechanical Engineering Congress and Exposition*, *50626*, V008T10A027.

Hågbo, T.-O., Giljarhus, K. E. T., Qu, S., & Hjertager, B. H. (2019). The performance of structured and unstructured grids on wind simulations around a high-rise building. *IOP Conference Series: Materials Science and Engineering*, *700*(1), 12001.

Holman, J. P. (2010). *Heat transfer* (TENTH EDIT). McGraw-Hill.

Jamal, A., El-Shaarawi, M. A. I., & Mokheimer, E. M. A. (2008). Effect of eccentricity on conjugate natural convection in vertical eccentric annuli. *HEFAT 2008*.

Jamal, A., & Mokheimer, E. (2022). Conjugate Natural Convection: A Study of Optimum Fluid Flow and Heat Transfer in Eccentric Annular Channels. *Journal of Engineering*, *2022*.

Laouira, H., Mebarek-Oudina, F., Hussein, A. K., Kolsi, L., Merah, A., & Younis, O. (2020). Heat transfer inside a horizontal channel with an open trapezoidal enclosure subjected to a heat source of different lengths. *Heat Transfer—Asian Research*, *49*(1), 406–423.

Mebarek-Oudina, F., Laouira, H., Aissa, A., Hussein, A. K., & El Ganaoui, M. (2020). Convection Heat Transfer Analysis in a Channel with an Open Trapezoidal Cavity: Heat Source Locations effect. *MATEC Web of Conferences*, *330*, 1006.

Multiphysics, C. (2013). Comsol multiphysics reference manual. *COMSOL: Grenoble, France*, *1084*, 834.

Mustafa, J., Siddiqui, M. A., & Anwer, S. F. (2019). Experimental and numerical analysis of heat transfer in a tall vertical concentric annular thermo-siphon at constant heat flux condition. *Heat Transfer Engineering*, *40*(11), 896–913.

PATIL, M. (2020). *AN INVESTIGATION INTO FLUID FLOW, HEAT AND MASS TRANSFER IN A VERTICAL POROUS ANNULAR CYLINDER WITH OUTER WALL SUBJECTED TO NATURAL CONVECTION.*

Roslan, R., Saleh, H., & Hashim, I. (2014). Natural convection in a differentially heated square enclosure with a solid polygon. *The Scientific World Journal*, *2014*.

Salih, N. M., Ezzat, S. B., Hassan, A. A., & Jasim, Q. K. (2021). Natural Convection in a Square Cavity Filled with Saturated Porous Media and Partially Heated From Below. *IOP Conference Series: Materials Science and Engineering*, *1094*(1), 12059.

Sankar, M., Park, J., & Do, Y. (2011). Natural convection in a vertical annuli with discrete heat sources. *Numerical Heat Transfer, Part A: Applications*, *59*(8), 594–615.

Seraji, M. H., & Khaleghi, H. (2019). A Numerical Study of the Effect of Aspect Ratio on Heat Transfer in an Annular Flow Through a 270-Degree Curved Pipe. *Journal of Chemical and Petroleum Engineering*, *53*(1), 101–110.

Sivasankaran, S., Do, Y., & Sankar, M. (2011). Effect of discrete heating on natural convection in a rectangular porous enclosure. *Transport in Porous Media*, *86*, 261–281.

Turan, O., Sachdeva, A., Poole, R. J., & Chakraborty, N. (2012). Laminar natural convection of power-law

fluids in a square enclosure with differentially heated sidewalls subjected to constant wall heat flux. *Journal of Heat Transfer*, *134*(12), 122504.

AUTHOR BIBLIOGRAPHY

Abrar A. S. Alhadad:
Master degree at mechanical engineering – power, University of Babylon, Iraq

Hussien M.Jassim:
Assistant prof. Dr. at college of engineering, Mechanical department, University of Babylon, Iraq
abraralhadad1@gmail.com